

Enhanced hole injection in a bilayer vacuum-deposited organic light-emitting device using a *p*-type doped silicon anode

X. Zhou, J. He, L. S. Liao, M. Lu, Z. H. Xiong, X. M. Ding, and X. Y. Hou^{a)}
Surface Physics Laboratory (National Key Laboratory), Fudan University, Shanghai 200433, China

F. G. Tao and C. E. Zhou
Chemistry Department, Fudan University, Shanghai 200433, China

S. T. Lee
Department of Physics and Material Science, City University, Hong Kong, China

(Received 12 October 1998; accepted for publication 16 November 1998)

We report the fabrication of a vacuum-deposited light-emitting device which emits light from its top surface through an Al cathode using *p*-type doped silicon as the anode material. Enhanced hole injection is clearly demonstrated from the *p*-Si anode as compared to the indium-tin-oxide (ITO) anode. The mechanisms of hole injection from both the *p*-Si and ITO anodes into the organic layer are investigated and a possible model based on anode surface band bending is proposed. During the operation of the organic light-emitting device, the surface band bending of the anode plays a very important role in modifying the interfacial barrier height between the anode and the organic layer.
© 1999 American Institute of Physics. [S0003-6951(99)01604-6]

Organic light-emitting devices (OLEDs) have attracted almost unprecedented attention in both the fields of fundamental research and device fabrication,¹⁻¹⁶ mainly because OLEDs have great potential for use in flat-panel displays.

Although ITO is an important material and is widely used as anodes in OLEDs, it also has some disadvantages as revealed in the previous literature.¹⁷⁻²¹ After the degradation of OLEDs, defects formed on the ITO surfaces have been observed using scanning electron microscopy.^{17,18} There is evidence that indium can diffuse into the organic materials.¹⁹⁻²¹ It has also been verified that ITO is inefficient in injecting holes into the polymers.²² To minimize the limitations of ITO, the introduction of the hole-transport layer prior to the deposition of the light-emitting layer and modifications of the ITO surface itself have also been extensively investigated.¹⁻⁶ In this letter, we use *p*-type Si instead of ITO as the anode to fabricate OLEDs. Enhanced hole injection from the *p*-type Si anode is clearly demonstrated. The mechanisms of hole injection from both *p*-Si and ITO have been investigated and a possible model based on the surface band bending of the anode at the interface has been proposed. The surface band bending can modify the interfacial barrier during the operation of OLEDs.

Because of the importance of Si-based optoelectronics, a few kinds of OLEDs fabricated on Si substrates have been reported in the literature.²³⁻²⁵ Among the reported work, only Parker and Kim²³ presented polymer light-emitting devices by using either *n*- or *p*-type silicon as the electrodes for the injection of electrons or holes. In other works,^{24,25} Si wafers were used as the substrates to support OLEDs with an inverted geometry in which the ITO was deposited on the top surface of the organic materials and the cathode contact was placed on the bottom.

The substrates used in the experiments were *p*-type

Si(100) wafers and ITO coated glass. The Si wafers had a resistivity of 10 Ω cm. The Si substrates were first cleaned in a sequence of ultrasonic rinses in acetone, ethanol, and deionized water for 10 min each, and then they were etched for 20 s in a 4% HF solution to remove the native oxide and preserve the hydrogen-terminated surfaces. Finally, the Si substrates after rinsing in the deionized water were blown dry by nitrogen gas. The glass substrates coated with 25-nm-thick ITO (with a sheet resistance of 77 Ω/\square) were cleaned by sequential ultrasonic rinses in detergent, acetone, ethanol, and deionized water for 10 min each. The cleaned Si wafers and ITO glasses were immediately loaded into an evaporation chamber with a base pressure of 10^{-5} Torr. The structure configurations of the fabricated OLEDs on both the ITO and Si substrates are shown in the inset of Fig. 1. The organic films were deposited at room temperature starting with a 40-nm-thick hole-transporting layer of *N,N'*-diphenyl-*N,N'*-bis(3-methylphenyl)-1,1'-biphenyl-4,4'-diamine (TPD), followed by a 40-nm-thick electron-transporting layer and light-emitting layer of aluminum tris(8-hydroxyquinoline) (Alq_3). Finally, an aluminum cathode electrode was deposited on the top of the organic materials in a separate chamber.

Figure 1 shows the forward-bias current-voltage characteristics of devices with *p*-type Si and ITO anodes, respectively, and are typical of the *I*-*V* data obtained from a group of sample OLEDs. There are significant differences in the current-voltage characteristics between the devices fabricated with *p*-type Si electrodes and similar devices fabricated with ITO electrodes. The devices with ITO anodes require a higher turn-on voltage than the devices with *p*-type Si anodes to reach a similar current density of 2 mA/cm². The turn-on voltage of ITO\TPD\Alq₃\Al is about 8 V, while that of Al\p-Si\TPD\Alq₃\Al is only 5 V. The devices with *p*-type Si anodes are able to generate a substantially larger current density at the same forward drive voltage compared to the

^{a)}Electronic mail: xyhou@srcap.stc.sh.cn

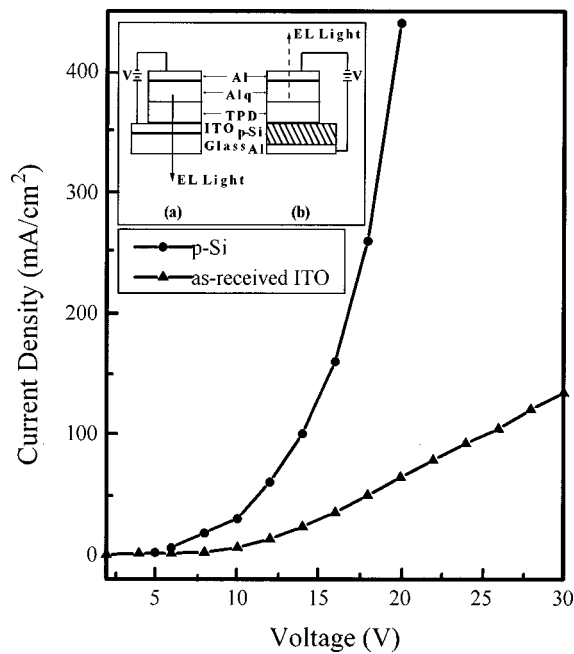


FIG. 1. Current–voltage characteristics of OLEDs using an ITO and a *p*-type Si anode. Inset: OLED structures (a) ITO/TPD/Al₃/Al and (b) Al/*p*-Si/TPD/Al₃/Al.

devices with ITO anodes. To achieve a current density of 130 mA/cm², the driving voltages for ITO/TPD/Al₃/Al and Al/*p*-Si/TPD/Al₃/Al are 30 and 15 V, respectively. These results clearly demonstrate enhanced hole injection from *p*-type Si anodes as compared with ITO anodes, because electron injection from the Al cathodes remains unchanged under forward-bias conditions. Devices with either *p*-Si or ITO as their anodes have a very small current flow in reverse bias and no light is observed.

For an ITO/TPD/Al₃/Al device, in a forward bias of 8 V, light is emitted with a brightness of 1 cd/m². The luminance of the device is 145 cd/m² at 16 V with a current density of 35 mA/cm². The luminance increases to 600 cd/m² at 30 V with a current density of 130 mA/cm². The light output is proportional to the current density, which is the same as the results reported in previous works.^{1–3} For Al/*p*-Si/TPD/Al₃/Al devices, we did not attempt to measure their luminescence at the beginning of the study because very thick (about 0.4 μm) Al electrodes were used in all of the fabricated devices and our emphasis was on the comparative study of *I*–*V* characteristics between devices with different anodes. However, uniform light can be also seen through the thick Al electrodes across the entire device area. Light emission through the Al electrodes are visible to the eye above a forward bias of 10 V and a current density of 30 mA/cm². The color emitted from the devices with *p*-Si is identical to that from the devices with ITO. The luminance of the devices is increased and measured to be about 0.5–0.8 cd/m² at 20 V with a current density of 440 mA/cm². After a simple correction of the transmission loss by a direct measurement of light decay through an Al film with a thickness exactly the same as that used in the Si-based OLEDs, there is a 10 000-fold reduction in light transmission through the thick Al electrode. Consequently, the intensity of the luminescence is estimated to be about 6500 cd/m², which is higher than that of the devices with ITO anodes. This implies

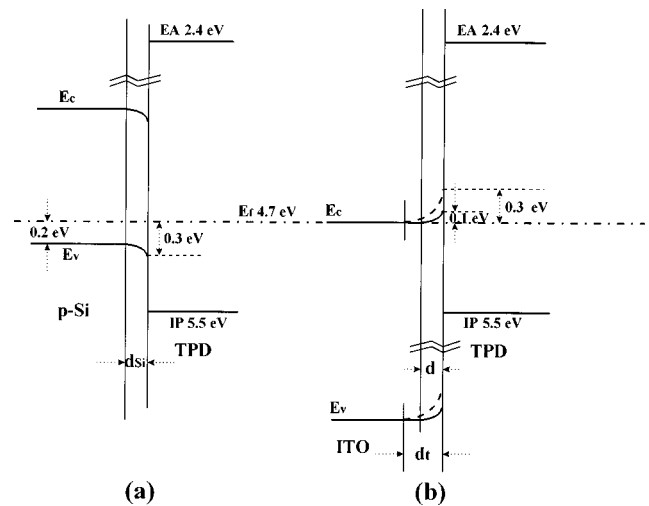


FIG. 2. Schematic band diagram of the (a) *p*-Si/TPD and (b) ITO/TPD interface.

that the internal quantum efficiency of the devices with *p*-Si is presumably higher than that of the devices with ITO. Since the typical thickness of the Al electrode is about 0.4 μm, the transmittance of light, the ratio I/I_0 of the transmitted light intensity *I* to the incident light intensity *I*₀, is calculated to be about 0.01% based on the equation $I/I_0 = \exp(-\alpha d)$, where *d* is the thickness of the Al film, α is the absorption constant defined as $\alpha = 4\pi k/\lambda$, and *k*, the extinction coefficient, is about 6.85 for Al at the wavelength λ of 0.52 μm.²⁶ This calculation shows that the light intensity through the Al is four orders of magnitude lower than the primary light intensity. Therefore, the calculated transmittance is in good agreement with the measured value.

One of the most important factors controlling the hole injection of a device is the interfacial electronic structure of the anode contact with the organic layer, TPD. We propose a possible model of band bending formation at the anode and organic layer interface to account for hole-injection behavior in OLEDs. An energy-level diagram for the Si(100)/TPD and ITO/TPD contacts is depicted in Fig. 2. The work function of both *p*-Si and ITO used here is the commonly cited value of 4.7 eV.^{22,23,27} The ionization potential (IP) and the electron affinity (EA) for TPD is 5.5 and 2.4 eV, respectively.²⁸ The surface Fermi level of *p*-type Si(100) is usually pinned at 0.3 eV,²⁹ above the top of the valence band, and consequently, results in the downward surface bending of about 0.1 eV, while the Fermi level in the bulk is located at about 0.2 eV above the top of the valence band due to its doping concentration. Although the band offset between the highest occupied molecular orbital (HOMO) of the TPD and the top of valence band in the bulk of the Si is 0.6 eV, the effective barrier for holes injected into the TPD at interface is only 0.5 eV due to the downward band bending of 0.1 eV at the surface (or interface). The band bending barrier of 0.1 eV will be compensated by the forward bias and will result in a barrier height of 0.5 eV as seen by the holes during the operation of the devices. ITO is a degenerate *n*-type semiconductor. Therefore, like conventional semiconductors such as Si, GaAs, and InP, there is a reasonable surface band bending upward at the *n*-type ITO surface. Even the width (*d* and *dt*) of the space-charge layer is much thinner in terms of

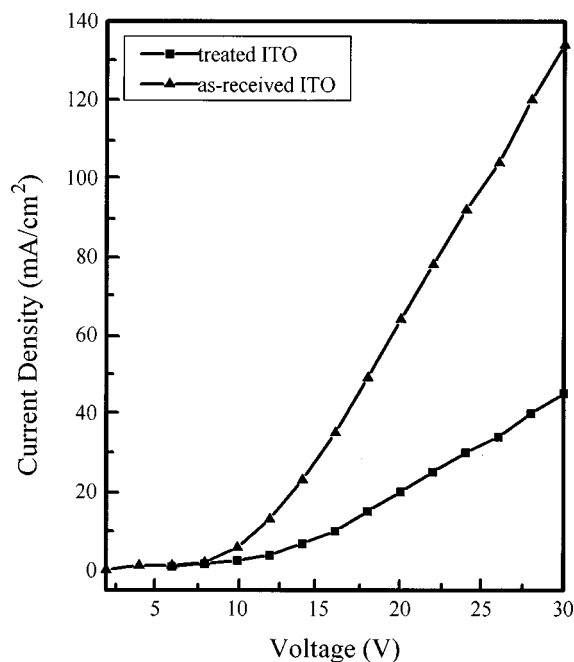


FIG. 3. Current–voltage characteristics of OLED devices using an as-received ITO and a treated ITO anode.

its degenerated feature. van den Meerakker *et al.*³⁰ characterized ITO films using (photo)electrochemical measurements in aqueous H_2SO_4 solutions and determined the flatband potential, or surface band bending, as a function of the charge-carrier concentration of ITO. They found that a decrease in the carrier concentration from 6×10^{20} to $1 \times 10^{20} \text{ cm}^{-3}$ resulted in a shift of 0.5 eV in the surface band bending. In Fig. 2(b), we assume that the surface band bending $E_c^s - E_f$ is about 0.1 eV due to its carrier concentration of $9.3 \times 10^{20} \text{ cm}^{-3}$, while $E_c - E_f$ is about 0.03 eV in the bulk.³¹ During the process of hole injection from ITO, the electron is emitted from the HOMO of the TPD to the empty states of the ITO near the Fermi level. Thus, the electrons see a barrier height of about 0.9 eV between the TPD and the conduction band of ITO. The barrier height of the holes for Si is 0.4 eV smaller than that for ITO, which accounts for the enhancement of hole injection for the *p*-type Si anodes as compared to the ITO anodes in the fabricated OLEDs.

The surface band bending of ITO increases with decreasing carrier concentration.³⁰ Subsequently, the hole-injection efficiency will be lower for ITO with a high resistivity because of a higher barrier height due to increased surface band bending. Figure 3 shows obvious differences in current–voltage characteristics between the OLEDs with as-received ITO and the OLEDs with treated ITO as the anode. The treated ITO, which has a charge-carrier concentration of $3.4 \times 10^{20} \text{ cm}^{-3}$, is prepared by rapid thermal annealing with O_2 flux of 5 L/min at 400 °C for 600 s. The sheet resistance of treated ITO is two times higher than that of as-received ITO. The surface band bending of the treated ITO is about 0.2 eV greater than the as-received ITO and the width of the space-charge layer also increases, which is depicted as a dash line in Fig. 2(b). The reduction of hole-injection efficiency for the treated ITO can be easily explained from the *I*–*V* characteristics as shown in Fig. 3. The light emission from the OLEDs with treated ITO also decreases. A decrease in

the carrier concentration of ITO results in a higher barrier height for hole injection into the TPD and, therefore, a lower hole-injection efficiency.

In summary, we have demonstrated light emission from OLEDs using doped *p*-Si as an anode material. Devices exhibit hole-injection characteristics different from those fabricated on ITO. This is explained in terms of a possible surface band bending model, which results in a different barrier height at the interface between the anode and the organic layer, TPD.

This work was supported by NSF of China with Grant Nos. 19525410 and 69776034.

- ¹C. W. Tang and S. A. VanSlyke, *Appl. Phys. Lett.* **51**, 913 (1987).
- ²C. W. Tang, S. A. VanSlyke, and C. H. Chen, *J. Appl. Phys.* **65**, 3610 (1989).
- ³S. A. VanSlyke, C. H. Chen, and C. W. Tang, *Appl. Phys. Lett.* **69**, 2160 (1996).
- ⁴C. C. Wu, C. I. Wu, J. C. Sturm, and A. Kahn, *Appl. Phys. Lett.* **70**, 1348 (1997).
- ⁵F. Li, H. Tang, J. Shinar, O. Resto, and S. Z. Weisz, *Appl. Phys. Lett.* **70**, 2741 (1997).
- ⁶S. Fujita, T. Sakamoto, K. Ueda, and K. Ohta, *Jpn. J. Appl. Phys., Part 1* **36**, 350 (1997).
- ⁷I. Sokolik, R. Priestley, A. D. Walser, R. Dorsinville, and C. W. Tang, *Appl. Phys. Lett.* **69**, 4168 (1996).
- ⁸V. Choong, Y. Park, Y. Gao, T. Wehrmeister, K. Müllen, B. R. Hsieh, and C. W. Tang, *Appl. Phys. Lett.* **69**, 1492 (1996).
- ⁹S. T. Lee, X. Y. Hou, M. G. Mason, and C. W. Tang, *Appl. Phys. Lett.* **72**, 1593 (1998).
- ¹⁰I. G. Hill, A. Rajagopal, A. Kahn, and Y. Hu, *Appl. Phys. Lett.* **73**, 662 (1998).
- ¹¹A. Rajagopal, C. I. Wu, and A. Kahn, *J. Appl. Phys.* **83**, 2649 (1998).
- ¹²V. E. Choong, Y. Park, N. Shivaparan, C. W. Tang, and Y. Gao, *Appl. Phys. Lett.* **71**, 1005 (1997).
- ¹³C. Adachi, K. Nagai, and N. Tamoto, *Appl. Phys. Lett.* **66**, 2679 (1995).
- ¹⁴A. Rajagopal and A. Kahn, *J. Appl. Phys.* **84**, 355 (1998).
- ¹⁵J. Kido, K. Hongawa, K. Okuyama, and K. Nagai, *Appl. Phys. Lett.* **68**, 217 (1996).
- ¹⁶N. Takada, T. Tsutsui, and S. Saito, *Appl. Phys. Lett.* **63**, 2032 (1993).
- ¹⁷P. E. Burrows, V. Bulovic, S. R. Forrest, L. S. Sapochak, D. M. McCarty, and M. E. Thompson, *Appl. Phys. Lett.* **65**, 2922 (1994).
- ¹⁸J. C. Scott, J. H. Kautman, P. J. Brock, R. DiPietro, J. Salam, and J. A. Goitia, *J. Appl. Phys.* **79**, 2754 (1996).
- ¹⁹A. R. Schlatmann, D. Wilms Floet, A. Hilberer, F. Garten, P. J. M. Smulders, T. M. Klawijk, and G. Hadziioannou, *Appl. Phys. Lett.* **69**, 1764 (1996).
- ²⁰E. Gautier, A. Lorin, J. M. Nunzi, A. Schalchli, J. J. Benattar, and D. Vital, *Appl. Phys. Lett.* **69**, 1071 (1996).
- ²¹Y. Hirose, Kahn, V. Aristov, and P. Soukiasian, *Appl. Phys. Lett.* **68**, 217 (1996).
- ²²I. D. Parker, *J. Appl. Phys.* **75**, 1656 (1994).
- ²³I. D. Parker and H. H. Kim, *Appl. Phys. Lett.* **64**, 1774 (1994).
- ²⁴D. R. Baigent, R. N. Marks, N. C. Greenham, R. H. Friend, S. C. Moratti, and A. B. Holmes, *Appl. Phys. Lett.* **65**, 2636 (1994).
- ²⁵V. Bulovic, P. Tian, P. E. Burrows, M. R. Gokhale, S. R. Forrest, and M. E. Thompson, *Appl. Phys. Lett.* **70**, 2954 (1997).
- ²⁶E. Shiles, T. Sasaki, M. Inokuti, and D. Y. Smith, *Phys. Rev. B* **22**, 1612 (1980).
- ²⁷Y. Park, V. Choong, Y. Gao, B. R. Hsieh, and C. W. Tang, *Appl. Phys. Lett.* **68**, 2699 (1996).
- ²⁸Y. Shirota, Y. Kuwabara, H. Inada, T. Wakimoto, H. Nakada, Y. Yonemoto, S. Kawami, and K. Imai, *Appl. Phys. Lett.* **65**, 808 (1994).
- ²⁹W. Mönch, *Semiconductor Surfaces and Interfaces* (Springer, Berlin, 1993).
- ³⁰J. E. A. M. van den Meerakker, E. A. Meulenlamp, and M. Scholten, *J. Appl. Phys.* **74**, 3282 (1993).
- ³¹J. C. C. Fan and J. B. Goodenough, *J. Appl. Phys.* **48**, 3524 (1977).